JOURNAL OF MATERIALS SCIENCE **38** (2003) 4081–4086

Micromechanical testing of MEMS materials

T. E. BUCHHEIT, S. J. GLASS, J. R. SULLIVAN, S. S. MANI
Sandia National Laboratories, Albuquerque, NM 87185, USA

D. A. LAVAN
Massachussetts Institute of Technology, Cambridge, MA 02139, USA

T. A. FRIEDMANN
Sandia National Laboratories, Albuquerque, NM 87185, USA

R. JANEK
Sandia National Laboratories, Livermore, CA 94550, USA

This paper discusses tensile testing techniques and results derived as part of a broader microstructure-properties investigation of structural materials used in surface micromachined (SMM), and LIGA MEMS technologies. SMM techniques produce devices on the surface of a silicon wafer, with critical dimensions as small as 1–2 μm, using a subtractive multilayer film deposition process. Two structural materials have been investigated: SUMMiT^{TM} polysilicon and amorphous Diamond (a-D). Mechanical properties presented in this paper on these SMM structural materials were obtained from a direct tensile testing method using the lateral force measurement capability of a nanoindentation system. LIGA, a German acronym extracted from the words "Lithographie, Galvanoformung, Abformung," is an additive process in which structural material is electrodeposited into a polymethyl-methacrylate (PMMA) molds realized by deep x-ray lithography. LIGA tensile specimens of several different materials have been evaluated using a mini-servohydraulic load frame, designed to test specimens of sizes similar to structural components. In this paper, tensile test results from LIGA fabricated Ni and Ni-alloys and examples of their correlation to processing and microstructure will be presented.

1. Introduction

Techniques for MEMS materials properties evaluation have developed concurrently with MEMS processing technologies. In recent years, several direct tensile testing techniques have been developed that test ligaments of structural material with gage sections as small as 2 × 2.5 microns [1–6]. This paper discusses two direct tensile testing methods and results for materials processed with two MEMS technologies: surface micromachining (SMM) and LIGA.

In the case of testing surface micromachined materials, a direct testing technique that uses the lateral loading capability of an MTS nanoindenter XP has been developed [5]. Specimens henceforth referred to as "pull-tabs" have been fabricated that can be engaged with an appropriately shaped nanoindenter tip. The simplest specimens contain a test ligament between a fixed end and pull ring end. When possible, specimens are designed with a pivot end rather than a fixed end to aid in alignment. A typical sample with a pivot end is illustrated in Fig. 1. To perform a test, the pull ring end is engaged with a flat bottomed tip fixed to a nanoindenter. The primary advantage of this technique is the ability to efficiently conduct many tests, thus providing strength data for statistical analysis, important to properties' characterization of brittle materials.

Several successful series of tests have been conducted on polysilicon, fabricated via Sandia National Laboratories' SUMMiT^{TM} processes, and amorphous diamond (a-D) pull-tabs [5]. The most recent results on a-D and on SUMMiT^{TM} polysilicon tabs testing using a flat-bottomed conical tip will be reviewed. Also, preliminary results on SUMMiT^{TM} polysilicon tabs tested with a cylindrical sapphire tip are presented and compared with the conical tip results. Although a statistical data set has not yet been obtained using the cylindrical tip, the data indicates that the new tip geometry offers an improvement in the testing technique.

LIGA component fabrication is a process in which structural material is electrodeposited into a patterned PMMA mold realized through deep X-ray photolithography [7, 8]. The process permits fabrication of metal micro-components that range from a few microns to several millimeters. LIGA processing is different than surface micromachining, but many consider LIGA a MEMS technology because of the small size scale and high precision of typical fabricated components. As with surface micromachine technology, methods for testing LIGA materials have developed with evolution of the technology [9, 10]. This paper includes selected results from a growing body of data on three Nickel-based LIGA fabricated materials, including Ni, Ni-Co, Ni-Fe. Results were obtained using a micromechanical

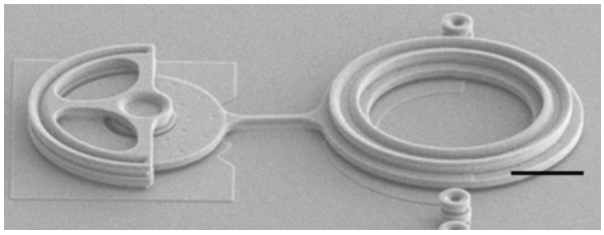

Figure 1 A typical polysilicon surface micromachined tensile specimen.

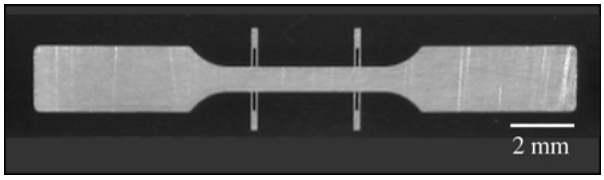

Figure 2 A typical LIGA fabricated tensile specimen.

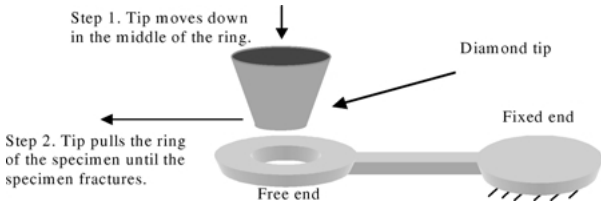

Figure 3 Schematic of surface micromachined pull-tab tensile test procedure.

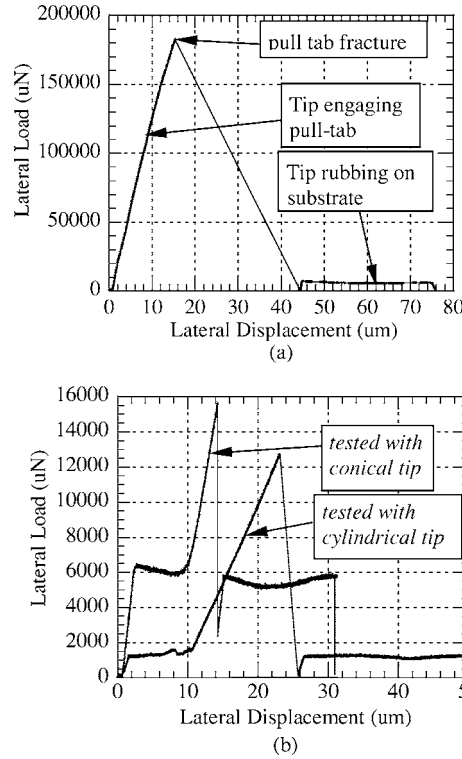

Figure 4 Lateral force vs. lateral displacement data from typical: (a) amorphous diamond (a-D) and (b) SUMMiT^{TM} polysilicon pull-tab experiments.

tensile test system developed specifically for evaluating LIGA materials [9]. The load frame accommodates a miniaturized version of a standard flat dog bone style tension test specimen with measurement tabs, used for gage section displacement measurement with a laser extensometer. A typical LIGA test specimen is illustrated in Fig. 2. Materials characterizations conducted on LIGA fabricated parts relevant to the mechanical properties testing are also presented in this paper.

2. Testing and results

2.1. Surface micromachined materials

A schematic of the test procedure used for surface micromachined materials is shown in Fig. 3. During an experiment, the flat bottom conical tip engages the pull ring end of the specimen and a normal force is applied to keep the tip engaged with the sample. The prescribed normal force is maintained throughout the experiment and recorded along with lateral force and lateral displacement. Typical lateral force vs. lateral displacement data is illustrated in Fig. 4. Fig. 4a illustrates an experiment using a flat bottomed conical tip to test an a-D pull-tab with a nominal gage section of 10 μm $\times$ 2 μm. Fig. 4b illustrates two experiments performed on polysilicon pull-tabs, one using the flat bottomed conical tip, and the other using a new cylindrical tip shown in figure 5. Locations where the tip is engaging the pull-tab, or simply making contact with the substrate surface beneath the pull-tab are easily distinguishable on the plots. To determine a fracture strength, lateral force data is offset by the amount of force required to drag the tip along the substrate surface then divided by the cross sectional area of the ligament. An additional geometrical correction accounting for the angle of engagement between the tip and the pull-tab is applied to data generated from tests using the conical tip [5].

The data shown in Fig. 4 illustrates two improvements over the original testing technique [5]. First, lateral displacement, used as the x-axis in Fig. 4, represents the difference between the relative motion of the nanoindenter column (in the real experiment the sample stage moves laterally while the column remains stationary) and the lateral tip deflection. The lateral tip deflection is measured by an optical system mounted within the nanoindenter column. Original published data using this technique plotted an ill-defined lateral displacement which was not simply relative column displacement and did not correctly account for tip deflection. The second improvement is enhanced normal force control. Normal force must be applied to maintain tip engagement with the pull-tab throughout the experiment. The normal force applied in previously published results [5, 6] typically exceeded 350 mN, a value that previously could not be carefully controlled, and resulted in a 20 mN frictional force caused by the tip rubbing against the substrate surface during the experiment. Data illustrated in Fig. 4 uses a normal force of 100 mN for the a-D pull-tab experiment, 75 mN for the polysilicon pull-tab experiment using the conical tip and 3 mN for the polysilicon pull-tab experiment using the cylindrical sapphire tip shown in Fig. 5. Each successively lower applied normal force resulted in a much lower frictional force. Referring to Fig. 4, the 100 mN normal force in the a-D pull-tab experiment resulted in a $\sim$10 mN frictional force. The 75 mN normal force

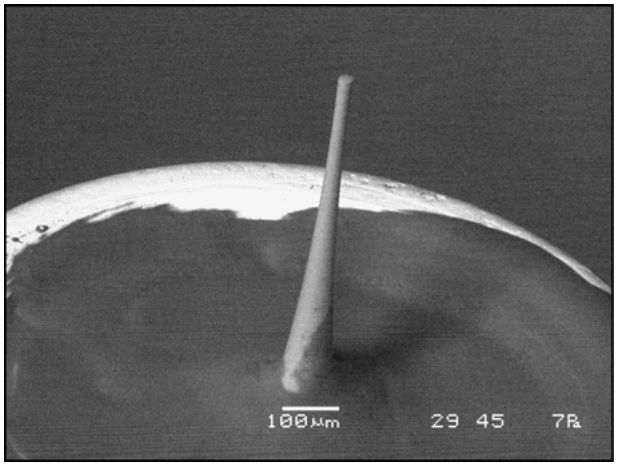

Figure 5 SEM image of cylindrical sapphire nanoindenter tip.

applied in the polysilicon pull-tab experiment using a conical tip resulted in a frictional force of 6 mN. The 3 mN normal force applied to the polysilicon pull-tab experiment which used the cylindrical tip resulted in a frictional force of less than 1 mN.

Fig. 4b illustrates a difference in compliance between a test performed using the cut-off conical tip and the cylindrical sapphire tip. The cylindrical sapphire tip adds compliance to the test configuration, as shown by the lower stiffness response measured during the engagement portion in the experiment in Fig. 4b. This additional compliance is thought to be from the relatively long and thin saphirre tip flexing during engagement with the pull tip. If this is the case, a more rigid cylindrical tip geometry should decrease the compliance of the test configuration. Also, a more rigid cylindrical tip may permit an additional reduction in normal force required for the tip to maintain engagement with the pull-tab during an experiment.

2.2. Surface micromachined polysilicon pull-tabs

Fig. 6 illustrates, in gray, the fracture strength distribution of ninety-seven 2 μm wide SUMMiT polysilicon pull-tabs using a flat-bottom conical tip [5]. The data set is compared with a smaller data set of pull-tab experiments using the cylindrical tip shown in Fig. 5. The x-axis in Fig. 6 represents failure probability, P, estimated by using the following equation [11]:

$$P = (j - 0.5)/n \tag{1}$$

where, n is the total number of samples, and j is the sample number when the sample data set is ranked in ascending order of fracture strength. Consistantly lower strengths were measured in the data set tested with the cylindrical tip.

A previous comparison of SUMMiT^{TM} polysilicon strength measurements using five independently developed methods revealed that using a conical tip and the lateral loading capability of a nanoindenter to test pull-tabs gave higher strengths when compared with the other four methods [6]. Results from this current study suggest that, in fact, using the conical tip may cause an error in the strength measurement. A reason for the error may be the angular engagement of the conical tip with the pull-tab. Although a correction was applied to account for the engagement angle [5], it is conceivable that the tip drives the tab into the substrate in a fashion that creates additional frictional force during the experiment. The cylindrical tip does not engage the pull-tab at an angle, thus will not tend to drive the pull-tab into the substrate. The results in Fig. 6 suggest that higher strength measurements in the experiments using the conical tip are caused by additional frictional force being captured in the measurement.

Tensile testing of pull-tabs using the lateral loading capability of a nanoindenter also provides an opportunity to measure Young's modulus of the ligaments. By testing pull-tabs of several different gage lengths, one can separate the system compliance from the pull-tab ligament compliance, i.e., the gage section compliance of the tension test. In turn, Young's modulus can be extracted from the gage section compliance. Previous attempts to extract the modulus from pull-tab tests using compliance correction did not provide consistent results. However, in the only case where the compliance of the pull-tab ligament was so much greater than the system compliance that the system compliance could be ignored, a Young's modulus value of 160 GPa was measured. This case was from a test on a pull-tab with 1000 μm long gage section.

Compliance corrected data obtained from pull-tab experiments using the cylindrical tip are given in Fig. 7. The corrected data is more consistent than that obtained using the conical tip, but still shows considerable scatter in specimens with gage sections less than 200 μm.

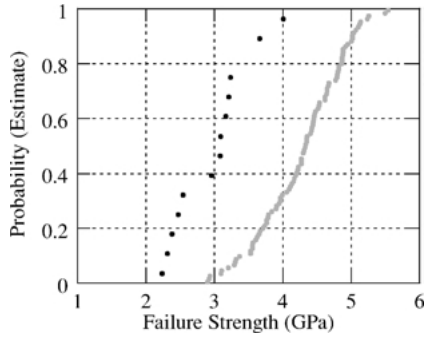

Figure 6 Failure Strength vs. Probability of SUMMiT^{TM} polysilicon pull-tabs tested using a conical and cylindrical tip.

2.3. Surface micromachined a-D pull-tabs

The a-D pull-tab is a fixed-end type design that resembles the schematic illustration in Fig. 3. Considerable strength data crossing a range of sample sizes have been collected from a-D pull-tab experiments. Fig. 7 illustrates the fracture strength data vs. gage volume and Fig. 8 provides a graphical Weibull analysis, where P represents the probability of failure, defined in Equation 1. The data reveals an obvious volume dependence and exhibits the probabilistic nature of failure commonly associated with brittle materials. SEM analyses

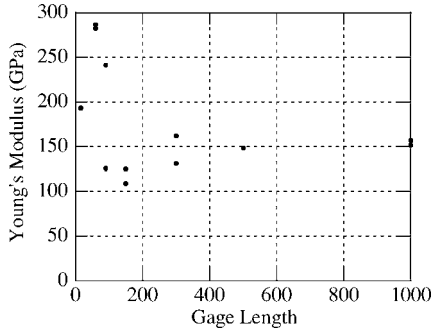

Figure 7 Compliance corrected Modulus vs. Gage Length data from SUMMiT^{TM} polysilicon pull tab tests using cylindrical tip.

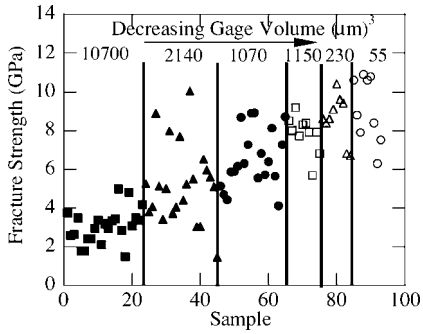

Figure 8 Fracture Strength vs. sample volume size data from a-D pull tab testing.

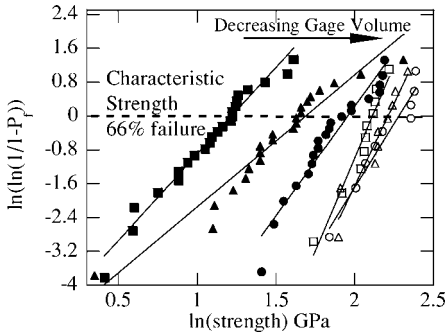

Figure 9 Weibull plot of a-D data.

of the fracture surfaces on larger gage section samples revealed two modes of fracture. One mode was associated with obvious defects on the surface of samples. The other mode was associated with edge defects thought to be caused by surface roughess. If a sample contained a processing defect, it failed at a lower strength. Samples with processing defects exhibited fracture strengths of less than 6 GPa whereas samples that failed at edge defects exhibited fracture strengths greater than 6 GPa. An example of each type of failure mode is illustrated in the SEM fractographs in Fig. 9. The figure illustrates mirror and hackle regions classically associated with brittle fracture. When these features were clearly delineated, quantitative fracture analyses of the experiments were performed.

2.4. LIGA mechanical testing

Fig. 11a shows tensile test results from LIGA Ni fabricated from sulfamate and Watts bath chemistries, and

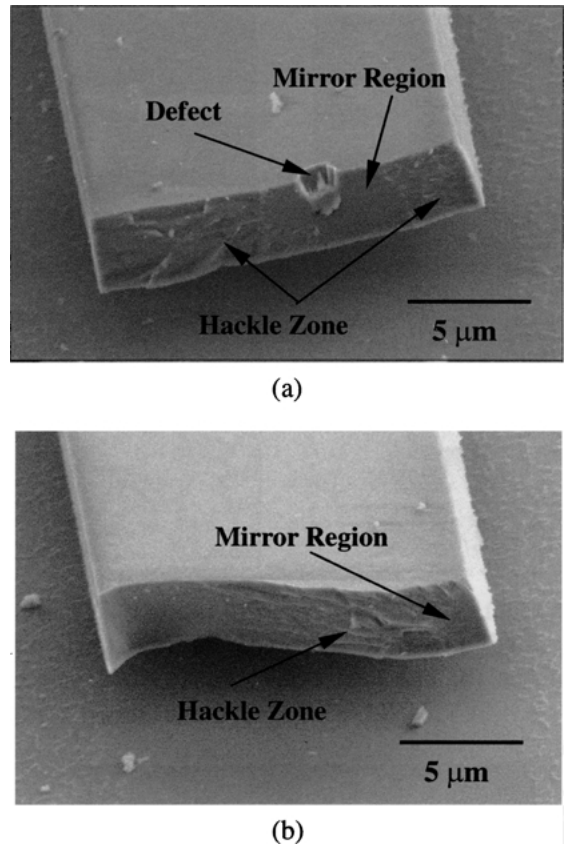

Figure 10 SEM micrographs of a-D fracture surfaces illustrating failure initiated by (a) a large defect and (b) a small edge defect.

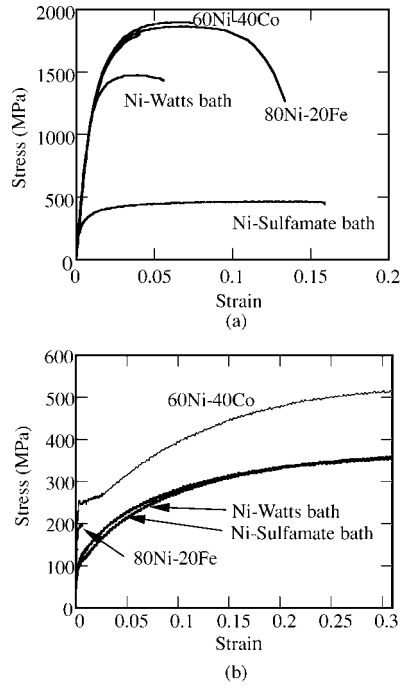

Figure 11 Tensile stress-strain response of (a) as-deposited and (b) annealed 700°C/1 h. LIGA fabricated materials.

two LIGA fabricated binary Ni-based alloys, 60%Ni-40%Co and 80%Ni-20%Fe. Fig. 11b shows the tensile stress-strain response of the same materials after a 700°C/1 h annealing treatment. The stress-strain curves in Fig. 11a show significant differences in the response of the LIGA Ni alloys relative to the pure LIGA Ni

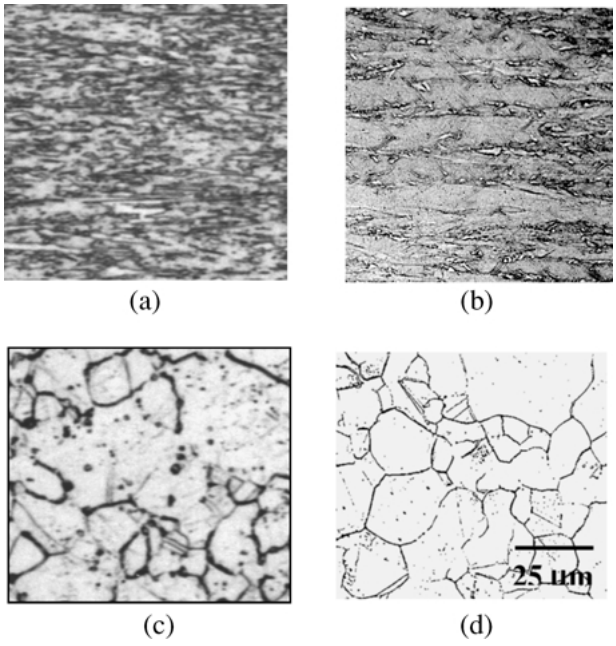

Figure 12 Optical micrographs of (a) as fabricated Watts bath, (b) as fabricated sulfamate bath, (c) annealed 700°C/1 h. Watts bath and (d) annealed 700°C/1 h. sulfamate bath LIGA Ni.

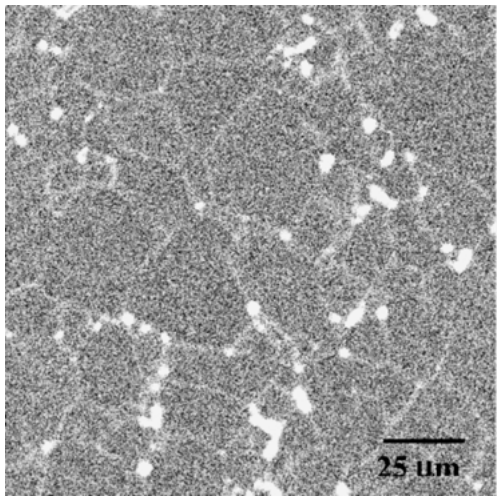

Figure 13 SEM microprobe Sulfur map in LIGA fabricated 80Ni-20Fe. Light-colored regions indicate sulfur concentrations.

and significant differences in the LIGA Ni deposited from different bath chemistries. These differences in mechanical response are attributable to processing and microstructure. In the case of LIGA Ni fabricated from the different bath chemistries, cross-section optical micrographs, illustrated in Fig. 13, show that the Watts bath nickel has a fine grain size relative to the sulfamate bath nickel. The micrographs indicate that the increased strength in Watts bath nickel resulted from the grain size refinement. The microstructural refinement in the Watts bath LIGA Ni, relative to the sulfamate bath LIGA Ni, was attributed to saccharin and coumarin additives present only in the Watts bath chemistry [12]. The differences in as-deposited microstructure and properties disappeared with annealing. LIGA Ni fabricated from the two different bath chemistries has an almost identical tensile stress-strain response after a 1 h annealing treatment at 700°C. Optical metallographs of annealed samples from both bath chemistries, illustrated in Fig. 11c–d, show that samples have similar microstructures with nearly identical grain sizes.

Tensile stress-strain curves of as-deposited 80Ni-20Fe and 60Ni-40Co exhibit significantly higher strengths than the as-deposited LIGA Ni. As with the LIGA Ni, microstructure and processing affect the stress-strain response of the LIGA Ni alloys. The microstructures of the LIGA Ni alloys in the as-fabricated condition were too fine to be revealed by optical metallography. TEM analyses were conducted on the LIGA 80Ni-20Fe alloy and suggested a grain size of approximately 100 nm. This further refinement in grain size contributed, at least in part, to the increased strength of the LIGA fabricated alloys relative to their pure Ni counterparts.

Annealing the alloys dramatically affected their mechanical response. The expected response to annealing is a decrease in strength and an increase in ductility. However, rather than exhibiting an increase in ductility, Fig. 11b shows that after the 700°C/1 h annealing treatment, the 80Ni-20Fe alloy embrittles to nearly 0% ductility. SEM microprobe analyses revealed the cause of the embrittlement. Fig. 13 illustrates a sulfur concentration map obtained from microprobe data. Concentrations of sulfur at the grain boundaries, indicated as light regions in Fig. 13, greatly weakens the boundaries causing the alloy to become susceptible to intergranular fracture at very low tensile strains.

Previous researchers have noted the deleterious effects of Sulfur in Ni-based electrodepositions [13]. The sulfur present in bath chemistry additives used to reduce the stress of the Ni-Fe deposition is co-deposited with the Ni and Fe. The as-deposited 80Ni-20Fe alloy does not experience deleterious effects from the presence of sulfur, because it is uniformly distributed within the deposition. Annealing is required to sweep the sulfur to grain boundaries through diffusion and grain growth processes.

The stress-strain curve of the LIGA fabricated + annealed 60Ni-40Co alloy shows a response more typical of annealed alloys, i.e., a decrease in tensile strength and a corresponding increase in ductility. After annealing, the LIGA Ni-Co alloy still retains a respectable yield strength suggesting this alloy may be useful in higher temperature applications. Also the annealed LIGA Ni-Co sample experiences yield point effects, common to solid solutions, suggesting some interaction between the cobalt solute atoms and defects in the alloy microstructure during the annealing treatment.

3. Conclusions

- A new cylindrical nanoindenter tip has been used to engage polysilicon "pull-tab" tensile samples. The cylindrical tip seems to overcome differences in fracture strength measurements previously obtained using the nanoindenter—pull-tab test method relative to other direct testing methods of MEMS polysilicon.
- Amorphous Diamond (a-D) pull-tab microtensile specimens showed failure distributions consistent with flaw distribuitions.

- LIGA fabricated Ni-Co, Ni-Fe and Watts Ni showed high strength, presumably due to the fine grain size of the materials.
- Sulfur incorporation into LIGA Ni-Fe materials during processing causes severe embrittlement of these alloys during annealing.

Acknowledgments

The authors acknowledge the assistance of Bonnie McKenzie, Alice Kilgo, David Schmale, Paul Hlava and Brad Boyce for their supporting efforts in preparing this manuscript. *Sandia is a multiprogram laboratory operated by Sandia Corporation, a Lockheed Martin Company, for the United States Department of Energy under Contract DE-ACO4-94AL85000.*

References

1. D. T. READ and J. C. MARSHALL, in SPIE Proceedings, (1996) Vol. 2880, p. 56.
2. T. TSUCHIYA, O. TABATA, J. SAKATA and Y. TAGA, Trans. Inst. Electr. Eng. Jpn. Part A **116-E**(10) (1996) 441.
3. W. N. SHARPE JR., B. YUAN and R. L. EDWARDS, Thin Films: Stress and Mechanical Properties VII, MRS Proceedings, Warrendale, PA, 1998, p. 51.
4. S. GREEK and F. ERICSON, Microelectromechanical Structures for Materials Research; MRS Proceedings, Vol. 518, Warrendale, PA, 1998.
5. D. A. LAVAN, K. JACKSON, S. J. GLASS, T. A. FRIEDMANN, J. P. SULLIVAN and T. E. BUCHHEIT, Mechanical Properties of Structural Films, ASTM STP 1413, American Society for Testing and Materials.
6. D. A. LAVAN, T. TSUCHIYA, G. COLES, W. G. KNAUSS, I. CHASIOTIS and D. READ, Mechanical Properties of Structural Films, ASTM STP 1413, American Society for Testing and Materials.
7. E. W. BECKER, W. EHREFELD, P. HAGMANN, A. MANER and D. MUNCHMEYER, Microelectr. Engin., **4** (1986) 35.
8. W. BACHER, W. MENZ and J. MOHR, *IEEE Trans. Ind. Electr.*, **42**(5) (1995) p. 431.
9. T. R. CHRISTENSON, T. E. BUCHHEIT and D. T. SCHMALE, *Mater. Sci. Microelectromech. Syst. (MEMS) Dev.*, **546** (1999) 127.
10. H. R. LAST, R. WITT and K. HEMKER, Microelectromech. Structures for MEMS Materials, MRS Proceedings, Vol. 605.
11. J. D. SULLIVAN and P. H. LAUZON, *J. Mater. Sci. Lett.* **5** (1986) 1245.
12. T. E. BUCHHEIT, D. A. LAVAN, J. R. MICHAEL, T. R. CHRISTENSON and S. D. LEITH, Metallurgical. Transactions A, 2001, accepted for publication.
13. J. A. BROOKS, J. W. DINI and H. R. JOHNSON, "Effects of Impurities on the Weldability of Electroformed Nickel" SAND78-8774, Sandia National Laboratories, 1978.